

See discussions, stats, and author profiles for this publication at: <https://www.researchgate.net/publication/235434752>

# Surface Modification of Colloidal TiO<sub>2</sub> Nanoparticles, with Bidentate Benzene Derivatives

ARTICLE in THE JOURNAL OF PHYSICAL CHEMISTRY C · JULY 2009

Impact Factor: 4.77 · DOI: 10.1021/jp9013338

---

CITATIONS

82

---

READS

31

## 4 AUTHORS, INCLUDING:



[Zoran Saponjic](#)

Vinča Institute of Nuclear Sciences

77 PUBLICATIONS 840 CITATIONS

SEE PROFILE



[Mirjana Comor](#)

Vinča Institute of Nuclear Sciences, Univer...

79 PUBLICATIONS 979 CITATIONS

SEE PROFILE



[Jovan M Nedeljković](#)

Vinča Institute of Nuclear Sciences

188 PUBLICATIONS 3,463 CITATIONS

SEE PROFILE

Surface Modification of Colloidal TiO<sub>2</sub> Nanoparticles with Bidentate Benzene Derivatives

Ivana A. Janković,\* Zoran V. Šaponjić, Mirjana I. Čomor, and Jovan M. Nedeljković

Laboratory for Radiation Chemistry and Physics, Vinča Institute of Nuclear Sciences, P.O. Box 522, 11001 Belgrade, Serbia

Received: February 13, 2009; Revised Manuscript Received: May 26, 2009

Surface modification of nanocrystalline TiO<sub>2</sub> particles (45 Å) with bidentate benzene derivatives, that is, 2-hydroxybenzoic acid, 2,5-dihydroxybenzoic acid, 2,3-dihydroxybenzoic acid, 3,4-dihydroxybenzoic acid, and catechol was found to alter optical properties of nanoparticles. The formation of the inner-sphere charge transfer (CT) complexes results in a red shift of the semiconductor absorption compared to unmodified nanocrystallites. The binding structures were investigated by using FTIR spectroscopy. The investigated ligands have the optimal geometry for chelating surface Ti atoms, resulting in ring coordination complexes (catecholate or salicylate type of binuclear bidentate binding), thus restoring six-coordinated octahedral geometry of surface Ti atoms. From the Benesi–Hildebrand plot, the stability constants at pH 2 of the order 10<sup>3</sup> M<sup>-1</sup> have been determined.

## 1. Introduction

The mechanism of semiconductor-assisted photoconversion is based on the principle that semiconductor nanoparticles behave as miniature photoelectrochemical cells.<sup>1–3</sup> The absorption of ultra-band-gap energy promotes an electron from the valence band to the conduction band, leaving a positively charged hole in the valence band. Most of the charge pairs recombine either radiatively or nonradiatively, while only a small fraction of the electrons and holes moves to the surface and either reacts by direct electron transfer with adsorbed compounds or migrates into midgap surface sites.<sup>4</sup> Although nanoparticulate TiO<sub>2</sub> is very effective from an energetic point of view, it is a relatively inefficient photocatalyst. The main energy loss is due to the recombination of charges generated upon excitation of TiO<sub>2</sub>, which is manifested as the relatively low efficiency of long-lived charge separation. In addition, due to its large band gap ( $E_g = 3.2$  eV), TiO<sub>2</sub> absorbs less than 5% of the available solar light photons. Hence, the main focus of research for the application of semiconductor-assisted photocatalysis is to improve both the separation of charges and the response in the visible spectral region.

To achieve enlarged separation distances, preventing the electron–hole recombination before desired redox reaction occurs, a TiO<sub>2</sub> nanoparticle surface was employed for establishing a strong coupling with electron-accepting or electron-donating species.<sup>5,6</sup> Consequently, the lifetime of charge separation and photocatalytic activity of TiO<sub>2</sub> nanoparticles are increased. The origin of the unique photocatalytic activities exhibited by TiO<sub>2</sub> nanoparticles comparing to the bulk is found in larger surface area with the existence of distorted surface sites. The techniques of X-ray absorption spectroscopy such as X-ray absorption near edge structure (XANES) and X-ray absorption fine structure (XAFS) are used to probe short-range structure of surface Ti sites in TiO<sub>2</sub> nanoparticles. It is well-known that, in the nanosize regime because of the large curvature of TiO<sub>2</sub> particles, the surface reconstructs in such a way that distorts the crystalline environment of surface Ti atoms

forming coordinatively unsaturated Ti atoms at the surface. The changes in the relative intensities and positions of characteristic peaks for TiO<sub>2</sub> nanoparticles ( $d < 20$  nm) in the pre-edge structure of the Ti K-edge spectrum (XANES) were observed confirming that the coordination of surface Ti atoms changes from octahedral (six-coordinate) to square-pyramidal (penta-coordinate).<sup>7</sup> The results obtained from measurements of XAFS spectra of these nanoparticles revealed the existence of shorter Ti–O bond lengths (1.79 Å) as compared to bulk anatase TiO<sub>2</sub> (1.96 Å).<sup>8</sup> These surface Ti atoms are very reactive and act as traps for photogenerated charges.<sup>9</sup> It was reported, on a whole class of electron-donating enediol ligands,<sup>6,10</sup> benzene derivatives,<sup>11</sup> or mercapto-carboxylic acids,<sup>12</sup> that binding to coordinatively unsaturated Ti atoms simultaneously adjusts their coordination to octahedral geometry at the surface of nanocrystallites and changes the electronic properties of TiO<sub>2</sub>. In such hybrid structures, localized orbitals of surface-attached ligands are electronically coupled with the delocalized electron levels from the conduction band of a TiO<sub>2</sub> semiconductor.<sup>13</sup> As a consequence, absorption of light by the charge-transfer (CT) complex yields to the excitation of electrons from the chelating ligand directly into the conduction band of TiO<sub>2</sub> nanocrystallites. This results in a red shift of the semiconductor absorption compared to that of unmodified nanocrystallites and enables harvesting of solar photons. Additionally, this type of electronic coupling yields to instantaneous separation of photogenerated charges into two phases, the holes localize on the donating organic modifier, and the electrons delocalize in the conduction band of TiO<sub>2</sub>. Moreover, the enediol ligands were found to act as conductive leads, allowing wiring of oligonucleotides and proteins resulting in enhanced charge separation and ensuing chemical transformations.<sup>14,15</sup>

In last two decades, the surface modification of commercial TiO<sub>2</sub> (Degussa P25,  $d \approx 30$  nm) with benzene derivatives (mainly catechol and salicylic acid) was studied.<sup>16–31</sup> Just few papers<sup>6,10–12,32</sup> investigated CT complex formation between enediol ligands and colloidal TiO<sub>2</sub> nanoparticles ( $d \approx 45$  Å), where binding of modifiers is stabilized by ligand-induced surface reconstruction of nanoparticles. In addition, a dilemma

\* To whom correspondence should be addressed. Tel: +381-11-8066428. Fax: +381-11-2453986. E-mail address: ivanaj@vinca.rs.

about  $\text{Ti}_{\text{surf}}$ –bidentate ligand CT complex composition exists: is it a mononuclear chelate or binuclear bridging complex?

Herein, we report surface modification of  $\text{TiO}_2$  nanoparticles with a whole class of enediol ligands (salicylic, 2,5-dihydroxybenzoic, 2,3-dihydroxybenzoic, 3,4-dihydroxybenzoic acid, catechol) that are able to adjust the coordination geometry of the surface Ti atoms inducing shift of the absorption onset toward the visible region of the spectrum, compared to unmodified nanocrystallites. Since these novel charge-transfer semiconducting materials exhibit optical properties that are distinct from their constituents, not absorbing in the visible region, Benesi–Hildebrand analysis for molecular complexes was employed to determine the stability constants from the absorption spectra. The stoichiometry of formed complexes was determined by using Job's method of continuous variation, and the result obtained proved both salicylate and catecholate types of binding are bidentate binuclear bridging complexes. The binding structures were investigated by using FTIR spectroscopy.

## 2. Experimental Methods

All the chemicals used were of the highest purity available and were used without further purification (Aldrich, Fluka). Milli-Q deionized water (resistivity  $18.2 \text{ M}\Omega \text{ cm}^{-1}$ ) was used as solvent. The colloidal  $\text{TiO}_2$  dispersions were prepared by the dropwise addition of titanium(IV) chloride to cooled water. The pH of the solution was between 0 and 1, depending on the  $\text{TiCl}_4$  concentration. Slow growth of the particles was achieved by using dialysis at  $4^\circ\text{C}$  against water until the pH 3.5 was reached.<sup>33</sup> The concentration of  $\text{TiO}_2$  (0.2 M) was determined from the concentration of the peroxide complex obtained after dissolving the colloid in concentrated  $\text{H}_2\text{SO}_4$ .<sup>34</sup> The mean particle diameter of titania used in this work was  $45 \text{ \AA}$ .

Surface modification of  $\text{TiO}_2$  resulting in the formation of a CT complex was achieved by the addition of surface-active ligands up to concentrations required to cover all surface sites ( $[\text{Ti}_{\text{surf}}] = [\text{TiO}_2]12.5/D$ ,<sup>35</sup> where  $[\text{Ti}_{\text{surf}}]$  is the molar concentration of surface Ti sites,  $[\text{TiO}_2]$  is the molar concentration of  $\text{TiO}_2$  in molecular units, and  $D$  is the diameter of the particle in  $\text{\AA}$ ). As the consequence of enhanced particle–particle interaction, upon surface modification that eliminates the surface charge, precipitation or “gelling” of the solution may occur. To avoid these problems pH of the solution was adjusted to 2 by diluting  $\text{TiO}_2$  or modifier stock solutions with 0.01 M aqueous solution of HCl. According to  $\text{pK}_a$  values known, carboxylic group in all ligands investigated is more than 90% in protonated form at pH 2. For the determination of CT complex binding constants, the absorption spectra were recorded at room temperature in cells with 1 cm optical path length using Thermo Scientific Evolution 600 UV/vis spectrophotometer.

In the application of continual variations method (Job's method)<sup>36</sup> for the spectrophotometric determination of the complex composition, the solutions were prepared by mixing some different volumes of equimolar solutions of 2 mM  $\text{Ti}_{\text{surf}}$  (7.2 mM  $\text{TiO}_2$ ) and 2 mM modifier. A series of solutions is prepared in which the sum of the total concentration of  $\text{Ti}_{\text{surf}}$  and modifier is constant (2 mM), but their proportions are continuously varied: volumes of  $\text{TiO}_2$  solution used varied from 1 to 9 mL and those of modifiers' solutions from 9 to 1 mL with the total volume being always 10 mL.

Infrared spectra were taken in attenuated total reflection (ATR) mode using a Nicolet 380 FTIR spectrometer equipped with a Smart Orbit ATR attachment containing a single-reflection diamond crystal. The angle of incidence was  $45^\circ$ . To avoid the precipitation of modified  $\text{TiO}_2$  and the excess of

unbound modifier, in the preparation of samples for FTIR measurements the quantity of ligands added was 50% of all  $\text{Ti}_{\text{surf}}$  sites ( $[\text{TiO}_2] = 0.2 \text{ M}$ ). The dispersions containing surface modified  $\text{TiO}_2$  nanoparticles were dried under argon at room temperature, and powders obtained were placed into the vacuum oven for 8 h to get to complete dryness. Before measuring FTIR spectra, powders were triturated in the agate mortar. Typically, 64 scans were performed for each spectrum with  $4 \text{ cm}^{-1}$  resolution. The spectrum of the dried  $\text{TiO}_2$  aqueous slurry (not containing modifier) was used as the background.

## 3. Results and Discussion

**3.1. Optical Properties of Surface Modified Nanocrystalline  $\text{TiO}_2$ .** When  $\text{TiO}_2$  particles are in the nanocrystalline regime, a large fraction of the atoms that constitute the nanoparticle is located at the surface with significantly altered electrochemical properties. As the size of nanocrystalline  $\text{TiO}_2$  becomes smaller than 20 nm the surface Ti atoms adjust their coordination environment from hexacoordinated (octahedral) to pentacoordinated (square pyramidal), which is followed by the compression of the Ti–O bond to accommodate for the curvature of the nanoparticle.<sup>7</sup> These undercoordinated defect sites are the source of novel enhanced and selective reactivity of nanoparticles toward bidentate ligand binding. All of the investigated ligands listed in Table 1, containing phenolic or carboxylic groups, were found to undergo binding at the surface (Figure 1), inducing new hybrid properties of the surface-modified nanoparticle colloids.

These hybrid properties arise from the ligand-to-metal charge transfer (CT) interaction coupled with electronic properties of the core of semiconductor nanoparticle. Consequently, the onset of absorption of these CT nanocrystallites is red-shifted compared to unmodified  $\text{TiO}_2$ . The shift in the absorption edge in the modified semiconductor nanoparticles is attributed to the excitation of localized electrons from the surface modifier into the conduction band continuum states of the semiconductor particle.<sup>10</sup> The optical shift induced by surface modification tuned by employing different surface-active ligands is shown in Figure 2, with the corresponding absorption onsets presented in Table 1. The lowest shift in the absorption edge position is obtained for 2-hydroxybenzoic acid (curve B) containing salicylate group ( $\text{COOH}$ ,  $\text{OH}$ ). The presence of additional hydroxyl group in para position in modifier molecule of 2,5-dihydroxybenzoic acid (curve C) induces further red shift which becomes more pronounced for 2,3-dihydroxybenzoic acid (curve D) and 3,4-dihydroxybenzoic acid (curve E) modifier molecules with OH groups in ortho position. The highest red shift in the absorption edge position is obtained for the catechol (curve F) containing two adjacent OH groups only.

The different position of the absorption threshold for these surface-modified nanoparticles is probably the consequence of changes in dipole moments of various surface bound Ti–ligand complexes.<sup>6</sup> Surface modification of  $\text{TiO}_2$  with benzoic acid having only carboxylic group does not lead to the shift of the absorption onset.<sup>13</sup> Apart from the shift in the absorption edge, the optical properties of surface modified semiconductor nanoparticles, having a continuous rise of absorption toward higher energies, paralleled the absorption properties characteristic of the band structure in bare semiconductor nanoparticles. A similar red shift, but in localized charge-transfer complex resulting in a pronounced absorption maximum, was previously observed for  $\text{Ti}^{4+}$  and catechol,<sup>37</sup> salicylic,<sup>38</sup> or ascorbic acid.<sup>39</sup>

It should be noted that all investigated enediol ligands are by themselves extremely susceptible to oxidation. Apparently,

**TABLE 1: Ligands Used for Modification of TiO<sub>2</sub> Nanoparticles, the Band Gaps upon Binding, and Benesi–Hildebrand Binding Constants**

ligand	label	structural formula	band gap, eV	$K_b$ , M <sup>-1</sup> a)
2-hydroxybenzoic acid	2-HBA		2.48	3300
2,5-dihydroxybenzoic acid	2,5-DHBA		2.13	2800
2,3-dihydroxybenzoic acid	2,3-DHBA		2.00	2800
3,4-dihydroxybenzoic acid	3,4-DHBA		2.00	2900
catechol	CAT		1.96	2500

<sup>a</sup> The absorption wavelengths at which the binding constants were determined are 375 nm (2-HBA), 400 nm (CAT), and 425 nm (2,3-DHBA, 2,5-DHBA, 3,4-DHBA). The stability constant  $K_b$  is determined with 3% error.

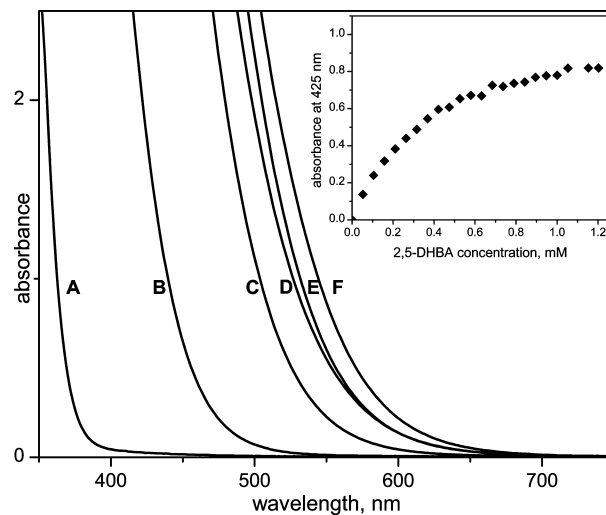


**Figure 1.** Colloidal solutions of 45 Å TiO<sub>2</sub> nanoparticles surface modified with different ligands: (A) bare TiO<sub>2</sub>, (B) 2-hydroxybenzoic acid, (C) 2,5-dihydroxybenzoic acid, (D) 2,3-dihydroxybenzoic acid, (E) 3,4-dihydroxybenzoic acid, and (F) catechol. Molecular structures are shown in Table 1.

because of the bidentate binding to nanoparticles, enediol ligands gain stability and are not easily oxidized. Endiol-modified TiO<sub>2</sub> colloids preserved their optical properties even after exposure to daylight for 2–3 months.

Because of the existence of undercoordinated surface defect sites and their lower efficiency of covalent bonding with solvent molecules in comparison with covalent bonding between atoms within the TiO<sub>2</sub> lattice, the surface species possess energy level in the midgap region.<sup>40</sup> Apart from red shift of the absorption onset of surface modified TiO<sub>2</sub> nanoparticles, charge transfer interaction between the molecule of modifier and surface Ti atoms also induces fine-tuning of the electrochemical potential of semiconductor nanocrystals indicating changes in oxidizing/reducing abilities.

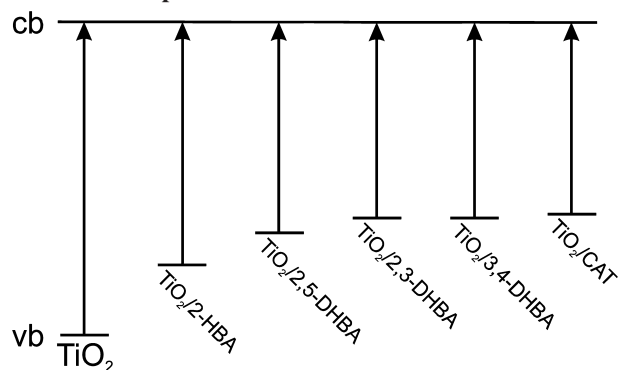
By extracting the corresponding onset/threshold energies from the absorption spectra of surface modified TiO<sub>2</sub> nanoparticles,



**Figure 2.** Absorption spectra of surface modified TiO<sub>2</sub> nanoparticles (0.09 M, pH 2) with different ligands (2.5 mM): (A) bare TiO<sub>2</sub>, (B) 2-hydroxybenzoic acid, (C) 2,5-dihydroxybenzoic acid, (D) 2,3-dihydroxybenzoic acid, (E) 3,4-dihydroxybenzoic acid, and (F) catechol. Inset: Absorption at 425 nm of TiO<sub>2</sub>–2,5-DHBA charge transfer complex vs modifier concentration (3.25 mM TiO<sub>2</sub>, data were recorded 20 h after surface modification).

the effective band gap energies ( $E = hc/\lambda$ ) of 2-HBA, 2,5-DHBA, 2,3-DHBA, 3,4-DHBA, and CAT modified TiO<sub>2</sub> nanoparticles at pH 2 were calculated to be 2.48, 2.13, 2.00, 2.00, and 1.96 eV, respectively (Chart 1). These results indicate similar electrochemical potentials of semiconducting nanocrystals modified with chosen class of enediol ligands indicating similar binding structures and effective electronic coupling. TiO<sub>2</sub> nanoparticles modified with these types of bidentate benzene derivatives can be used for development of dye-sensitized



**CHART 1: Energy-Level Positions Associated with Surface Modified TiO<sub>2</sub> Nanoparticles Obtained from the Shifts in Absorption Thresholds**


nanoporous titania solar cells where the dyes bind to the particles surface through carboxylic acid groups or enediol groups.<sup>41</sup> In addition, blends of surface modified TiO<sub>2</sub> nanoparticles and organic semiconductors cast from cosolutions can be used for synthesis of hybrid solar cells combining the unique properties of inorganic semiconductor and film-forming properties of polymers.<sup>42</sup>

**3.2. Determination of Stability Constants.** Since these novel charge-transfer semiconducting materials exhibit optical properties that are distinct from their constituents, not absorbing in the visible region, Benesi–Hildebrand analysis for molecular complexes<sup>43,44</sup> can be employed to determine the stability constant of CT complex. Benesi–Hildebrand analysis can be used for small particles since the same relationship is obtained between the stability constant and ligand concentration from Langmuir isotherm used for bulk compounds.<sup>6</sup> For a colloidal solution of 45-Å TiO<sub>2</sub>, one can consider the formation of an inner-sphere CT complex



with the stability constant  $K_b$  expressed as

$$K_b = \frac{[\text{CT}_{\text{complex}}]}{[\text{Ti}_{\text{surf}}][\text{L}]} \quad (2)$$

Since the absorption in the visible region originates solely from the complex formed it is obvious that  $[\text{CT}_{\text{complex}}] = A/\epsilon l$  and the eq 2 can be rearranged to the following linearized form

$$\frac{1}{A} = \frac{1}{K_b A_{\text{max}}} \frac{1}{[\text{L}]} + \frac{1}{A_{\text{max}}} \quad (3)$$

where  $[\text{L}]$  is the concentration of ligand and  $A$  and  $A_{\text{max}}$  are the absorbances of a CT complex for a given concentration of ligand  $L$  and saturation concentration corresponding to the full coverage of TiO<sub>2</sub> surface, respectively.

Stability constants  $K_b$  were determined from the absorbances of a series of solutions (Figure 2, inset) containing a fixed concentration of TiO<sub>2</sub> nanoparticles ( $C_{\text{TiO}_2} = 3.25$  mM, that is, 0.9 mM  $\text{Ti}_{\text{surf}}$ ) and increasing concentrations of ligands ( $C_{\text{ligand}} = 0.05$ –1.2 mM). To avoid great errors in  $K_b$  determination, the wavelength of complex absorption is chosen for each ligand to correspond to the requested absorption range ( $0.1 < A < 0.9$ ).<sup>44</sup>

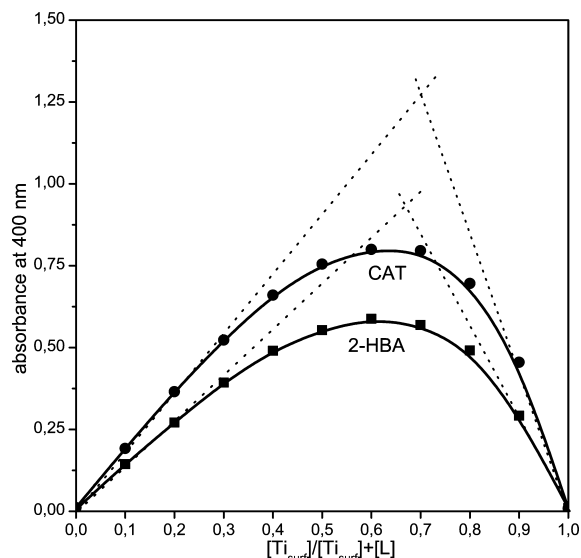


**Figure 3.** Job's curve of equimolar solutions for ligand–Ti<sub>surf</sub> complex;  $[\text{Ti}_{\text{surf}}] + [\text{L}] = 2$  mM.

By plotting  $1/A$  versus  $1/[\text{L}]$ , we obtained the straight lines, and from the ratio of the intercept and the slope,  $K_b$  values were determined and presented in Table 1. According to groups that participate in the binding to Ti<sub>surf</sub> (carboxylic, phenolic), from the molecular structures of ligands used it can be concluded that two types of binding may appear, salicylate (COOH, OH) or catecholate type (OH, OH). However, it is quite obvious that by comparing the measured values of  $K_b$  one cannot differentiate between these two types of binding since these values are similar, on the order  $10^3$  M<sup>−1</sup>. In the literature, to determine the CT complex stability constants for 2-HBA or CAT the adsorption approach after filtration method<sup>11,17–19,25</sup> or FTIR measurements<sup>23,24,26,27</sup> have been used, and  $K_b$  values of the order  $10^4$  M<sup>−1</sup> were reported. The discrepancy between  $K_b$  values may arise from the difference in the particle diameter or different methods used. In addition, our values may be underestimated since they were determined from only adsorption curves, although Benesi–Hildebrand method requires equilibrium conditions in which the rates of adsorption and desorption are equal.<sup>6</sup>

Additionally, the stoichiometric ratio between Ti<sub>surf</sub> atoms and modifiers in the CT complexes was checked by Job's method of continuous variation<sup>36</sup> assuming that only one type of complex is present in solution. According to Job's method the stoichiometric ratio ( $n$ ) is determined from the plot of the absorbance as a function of the mole fraction ( $x$ ) of metal or ligand. The ratio  $x_{\text{max}}/1 - x_{\text{max}}$ , where  $x_{\text{max}}$  corresponds to the mole fraction in the absorbance maximum, equals stoichiometric ratio ( $n$ ). The stoichiometric ratio Ti<sub>surf</sub>/modifier is obtained by plotting the absorbance of the CT complex versus  $x = [\text{Ti}_{\text{surf}}]/([\text{Ti}_{\text{surf}}] + [\text{L}])$ . Characteristic Job's curves for CAT and 2-HBA are presented in Figure 3. Job's plots for both complexes reached a maximum value at a mole fraction of  $[\text{Ti}_{\text{surf}}]/([\text{Ti}_{\text{surf}}] + [\text{L}]) \approx 0.67$ , confirming that molar ratio between Ti<sub>surf</sub> atoms and ligands in the complex is 2:1. The same Ti<sub>surf</sub>/ligand molar ratio was obtained for all other modifiers used.

**3.3. Binding Structure of Ligands at Nanoparticle Surface.** The way ligands bind to TiO<sub>2</sub> surface was investigated by using ATR-FTIR spectroscopy. Since the infrared spectrum of dried TiO<sub>2</sub> has only the characteristic broadband in 3700–2000 cm<sup>−1</sup> region,<sup>6</sup> we were able to measure spectra of modified colloids in 1750–1000 cm<sup>−1</sup> region, where the characteristic

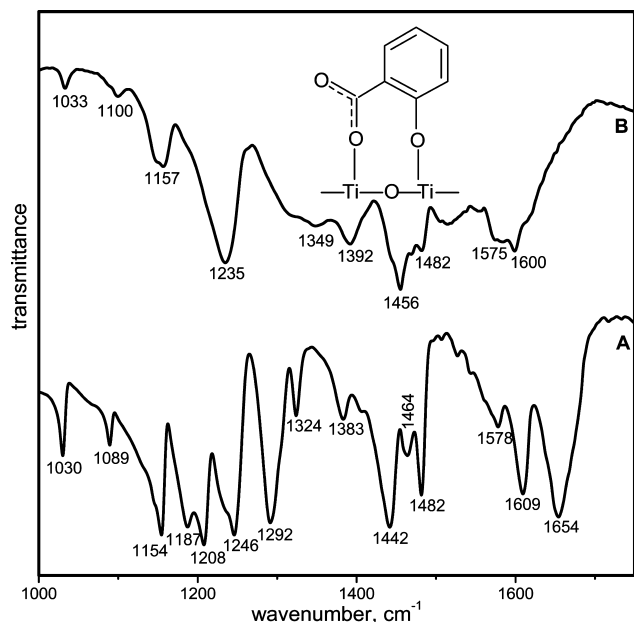


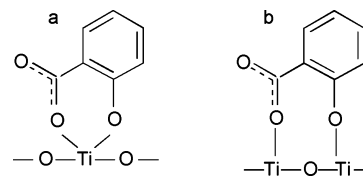
**Figure 4.** FTIR spectra of 2-HBA: free (A) and adsorbed on TiO<sub>2</sub> nanoparticles (B) with proposed binding structure.

bands of modifiers exist. Spectra of adsorbed ligands were obtained by subtracting the spectrum of bare TiO<sub>2</sub> nanoparticles from the spectrum of surface modified TiO<sub>2</sub> nanoparticles.

The ATR-FTIR spectra of 2-hydroxybenzoic (salicylic) acid, free and adsorbed on TiO<sub>2</sub> nanoparticles, were presented in Figure 4. The main bands and their assignments<sup>24,29,45–47</sup> in free (protonated) acid (curve A) are as follows: stretching vibrations of the aromatic ring  $\nu(\text{C}-\text{C})/\nu(\text{C}=\text{C})$  at 1609, 1578, 1482, 1464, and 1442 cm<sup>-1</sup>, stretching vibrations of the phenolic group  $\nu(\text{C}-\text{OH})$  at 1246 cm<sup>-1</sup>, bending vibrations of the phenolic group  $\delta(\text{C}-\text{OH})$  at 1383, 1324, 1208, and 1187 cm<sup>-1</sup>, bending  $\delta(\text{C}-\text{H})$  at 1154, 1089, and 1030 cm<sup>-1</sup>, stretching vibrations of CO in COOH  $\nu(\text{CO}/\text{COOH})$  at 1208 and 1187 cm<sup>-1</sup> (both bands are coupled with  $\delta(\text{C}-\text{OH})$ ), bending vibrations of CO in COOH  $\delta(\text{CO}/\text{COOH})$  at 1292 cm<sup>-1</sup>, and pronounced stretching vibration of the carbonyl group  $\nu(\text{C}=\text{O})$  at 1654 cm<sup>-1</sup>, existing only in the protonated form of acid.<sup>29,45</sup> The adsorption of 2-hydroxybenzoic acid onto TiO<sub>2</sub> nanoparticles (curve B) leads to complete disappearance of the bands at 1654, 1324, 1292, 1208, and 1187 cm<sup>-1</sup> and the shift of the band at 1246 cm<sup>-1</sup> to the lower frequency band at 1235 cm<sup>-1</sup>. Since these bands correspond to vibrations of phenolic OH and carboxylic COOH group, it is obvious that both groups take part in chelation of titanium atoms. The appearance of bands at 1575 and 1392/1349 cm<sup>-1</sup> doublet that can be attributed to carboxylate asymmetric and symmetric stretching vibrations,<sup>29,45</sup> respectively, as well as the disappearance of stretching vibration of the carbonyl group  $\nu(\text{C}=\text{O})$  at 1654 cm<sup>-1</sup> approve the deprotonation of COOH group as the consequence of its binding to Ti atoms with the formation of delocalized carboxylate group.<sup>48</sup> Ring frequencies are also affected by the new environment, that is,  $\nu(\text{C}-\text{C})/\nu(\text{C}=\text{C})$  bands are changed, indicating that binding makes different electronic distribution propagating to the whole aromatic ring. It is reported that charge transfer complex formed may be bidentate mononuclear chelate (Chart 2a) or bidentate binuclear bridging complex (Chart 2b).<sup>11,16,19,23,24,28–30,45,46,48</sup>

Since the value of  $\Delta\nu(\text{CO}_2^-) = \nu(\text{CO}_2^-)_{\text{asym}} - \nu(\text{CO}_2^-)_{\text{sym}} = 183/226 \text{ cm}^{-1}$  obtained is nearly the same as in the case of free salicylate,<sup>29,45</sup>  $\Delta\nu(\text{CO}_2^-) = 185/229 \text{ cm}^{-1}$ , bidentate binuclear (bridging) complex is formed. This conclusion is

**CHART 2: Proposed Coordination Structures for Salicylate Type of Binding**



approved by the result obtained from the Job's curve (Figure 3) where molar ratio between Ti<sub>surf</sub> atoms and 2-HBA in the complex is 2:1 (Chart 2, b).

The ATR-FTIR spectra of 2,5-dihydroxybenzoic (gentisic) acid, free and adsorbed on TiO<sub>2</sub> nanoparticles were presented in Figure 5. The assignments of main bands<sup>49,50</sup> in free (protonated) acid (curve A) are as follows: stretching vibrations of the aromatic ring  $\nu(\text{C}-\text{C})/\nu(\text{C}=\text{C})$  at 1623, 1610, 1593, 1496, 1472, and 1440 cm<sup>-1</sup>, stretching vibrations of the phenolic group  $\nu(\text{C}-\text{OH})$  at 1276 and 1237 cm<sup>-1</sup>, bending vibrations of the phenolic group  $\delta(\text{C}-\text{OH})$  at 1379, 1317, and 1186 cm<sup>-1</sup>, bending  $\delta(\text{C}-\text{H})$  at 1136 and 1076 cm<sup>-1</sup>, stretching and/or bending vibrations of CO in COOH at 1276, 1237, and 1186 cm<sup>-1</sup> (bands are coupled with  $\nu(\text{C}-\text{OH})$  or  $\delta(\text{C}-\text{OH})$ ), and pronounced stretching vibration of the carbonyl group  $\nu(\text{C}=\text{O})$  at 1668 cm<sup>-1</sup>. The adsorption of 2,5-dihydroxybenzoic acid onto TiO<sub>2</sub> nanoparticles (curve B) leads to the disappearance of the bands assigned to stretching and bending vibrations of phenolic OH and carboxylic COOH group at 1379, 1276, 1237, and 1186 cm<sup>-1</sup> with the formation of pronounced new band at 1210 cm<sup>-1</sup>, as well as the disappearance of the band assigned to stretching vibration of carbonyl group in COOH at 1668 cm<sup>-1</sup>. It may be concluded that both phenolic and carboxylic group take part in chelation of titanium atoms, as in the case of salicylic acid. Two bands of very low intensity between 1210 and 1338 cm<sup>-1</sup> could be assigned to vibrations of 5-OH group not bound to the surface, but since in this region coupling of vibrations of different groups exist, such conclusion cannot be drawn clearly.

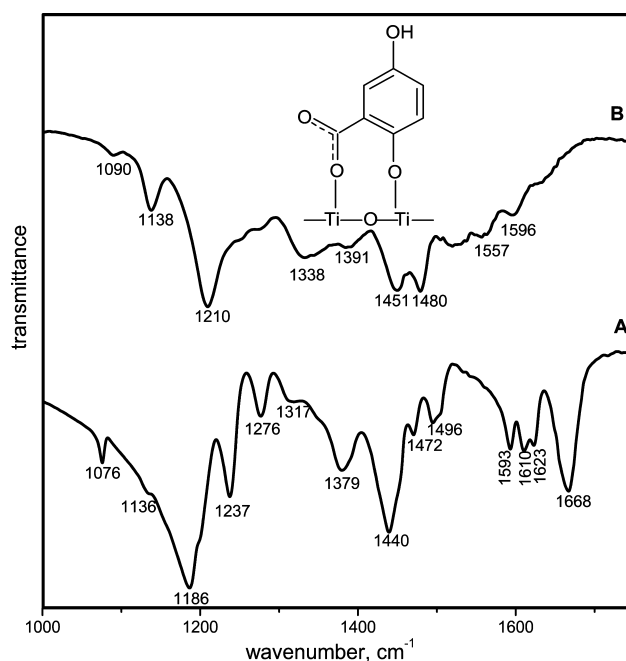


**Figure 5.** FTIR spectra of 2,5-DHBA: free (A) and adsorbed on TiO<sub>2</sub> nanoparticles (B) with proposed binding structure.

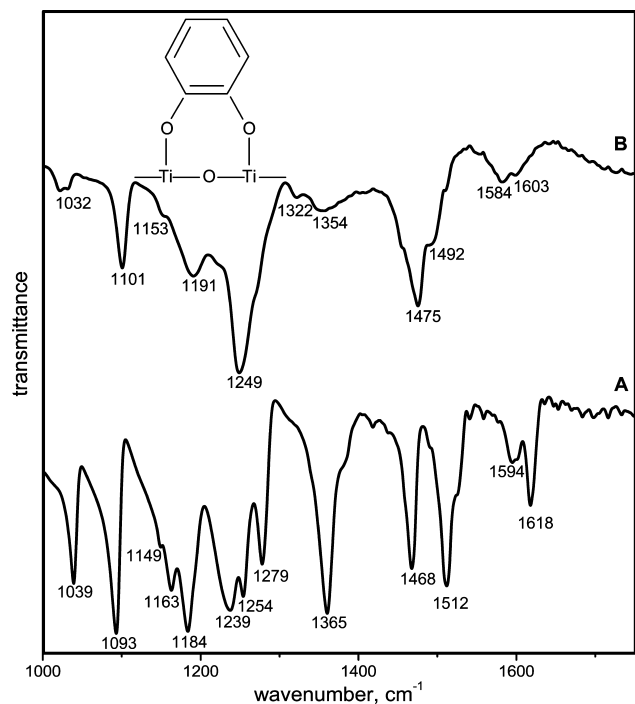


**Figure 6.** FTIR spectra of CAT: free (A) and adsorbed on TiO<sub>2</sub> nanoparticles (B) with proposed binding structure.

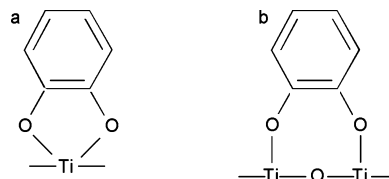
The formation of the charge transfer complex also affects the ring frequencies, that is,  $\nu(\text{C}-\text{C})/\nu(\text{C}=\text{C})$  bands in the region of 1400–1500 cm<sup>-1</sup> are shifted with change of intensity. The appearance of bands at 1557 and 1391/1338 cm<sup>-1</sup> doublet that can be attributed to carboxylate asymmetric and symmetric stretching vibrations,<sup>49</sup> respectively, as well as the disappearance of stretching vibration of the carbonyl group  $\nu(\text{C}=\text{O})$  at 1668 cm<sup>-1</sup> approve the deprotonation of COOH group upon binding to Ti atoms with the formation of delocalized carboxylate group.<sup>48</sup>

The value of  $\Delta\nu(\text{CO}_2^-) = \nu(\text{CO}_2^-)_{\text{asym}} - \nu(\text{CO}_2^-)_{\text{sym}} = 166/219$  cm<sup>-1</sup> obtained is nearly the same as in the case of free salicylate,<sup>29,45</sup>  $\Delta\nu(\text{CO}_2^-) = 185/229$  cm<sup>-1</sup>. The same way of binding as was proposed for 2-HBA (bridging complex) is quite expected having in mind molecular structures for these modifiers. This conclusion may also be approved by the result obtained from the Job's curve where molar ratio between Ti<sub>surf</sub> atoms and 2,5-DHBA in the complex was found to be 2:1 (not presented in Figure 3).

The ATR-FTIR spectra of catechol, free and adsorbed on TiO<sub>2</sub> nanoparticles were presented in Figure 6. The main bands and their assignments<sup>26,27,31</sup> in free catechol (curve A) are as follows: stretching vibrations of the aromatic ring  $\nu(\text{C}-\text{C})/\nu(\text{C}=\text{C})$  at 1618, 1594, 1512, and 1468 cm<sup>-1</sup>, stretching vibrations of the phenolic group  $\nu(\text{C}-\text{OH})$  at 1279, 1254, and 1239 cm<sup>-1</sup>, bending vibrations of the phenolic group  $\delta(\text{C}-\text{OH})$  at 1365, 1184, 1163, and 1149 cm<sup>-1</sup>, and bending  $\delta(\text{C}-\text{H})$  at 1039 and 1093 cm<sup>-1</sup>.

Upon adsorption of catechol onto TiO<sub>2</sub> (curve B), the difference between FTIR spectra of free and adsorbed modifier appears, indicating surface complexation with catechol bound to the oxide surface in bidentate form.<sup>26,27</sup> Bending  $\delta(\text{C}-\text{OH})$  vibrations in the region below 1200 cm<sup>-1</sup> lose their hyperfine structure, while the pronounced band at 1365 cm<sup>-1</sup> nearly disappears and a very weak and broad feature centered at 1354 cm<sup>-1</sup> appears. Three bands of stretching vibrations  $\nu(\text{C}-\text{OH})$  merge to one prominent band at 1249 cm<sup>-1</sup>. The binding of

### CHART 3: Proposed Coordination Structures for Catecholate Type of Binding



catechol to TiO<sub>2</sub> via two adjacent phenolic groups even affects the stretching of the aromatic ring (bands above 1400 cm<sup>-1</sup>).

Catecholate type of binding inherent to CAT molecule adsorption to metal-oxide surfaces, with two adjacent phenolic OH groups taking part in complexation, was reported to result in the formation of both bidentate mononuclear chelating (Chart 3a) and bidentate binuclear bridging (Chart 3b) complexes. There are two opinions dealing with catecholate binding: some authors<sup>6,51,52</sup> claim that five-membered ring coordination complexes predominate, while the others<sup>13,17,18,26,27</sup> find bridging complexes energetically more favorable. Since according to Job's curve the molar ratio between Ti<sub>surf</sub> atoms and catechol in the complex is 2:1 (Figure 3), the CT complex formed is most likely bidentate binuclear (bridging) complex (Chart 3b).

The ATR-FTIR spectra of 3,4-dihydroxybenzoic (protocatechuic) acid, free and adsorbed TiO<sub>2</sub> nanoparticles, were presented in Figure 7. The assignments of main bands<sup>49,53</sup> in free (protonated) acid (curve A) are as follows: stretching vibrations of the aromatic ring  $\nu(\text{C}-\text{C})/\nu(\text{C}=\text{C})$  at 1597, 1527, and 1419 cm<sup>-1</sup>, stretching vibrations of the phenolic group  $\nu(\text{C}-\text{OH})$  at 1273 and 1245 cm<sup>-1</sup>, bending vibrations of the phenolic group  $\delta(\text{C}-\text{OH})$  at 1394, 1341, 1286, and 1186 cm<sup>-1</sup>, bending vibrations  $\delta(\text{C}-\text{H})$  at 1128, 1120, and 1094 cm<sup>-1</sup>, stretching or bending vibrations of CO in COOH at 1273, 1245, 1220, and 1186 cm<sup>-1</sup>, and pronounced stretching vibration of the carbonyl group  $\nu(\text{C}=\text{O})$  at 1666 cm<sup>-1</sup>. The adsorption of 3,4-dihydroxybenzoic acid onto TiO<sub>2</sub> nanoparticles (curve B)

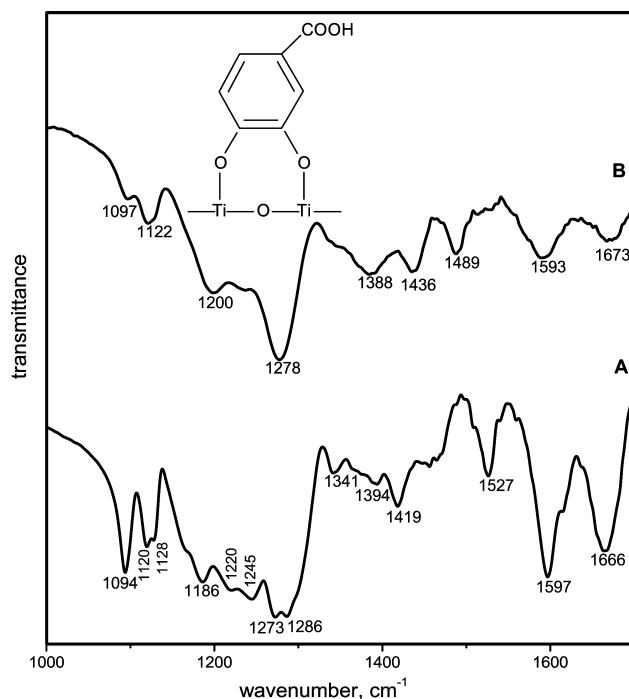


**Figure 7.** FTIR spectra of 3,4-DHBA: free (A) and adsorbed on TiO<sub>2</sub> nanoparticles (B) with proposed binding structure.



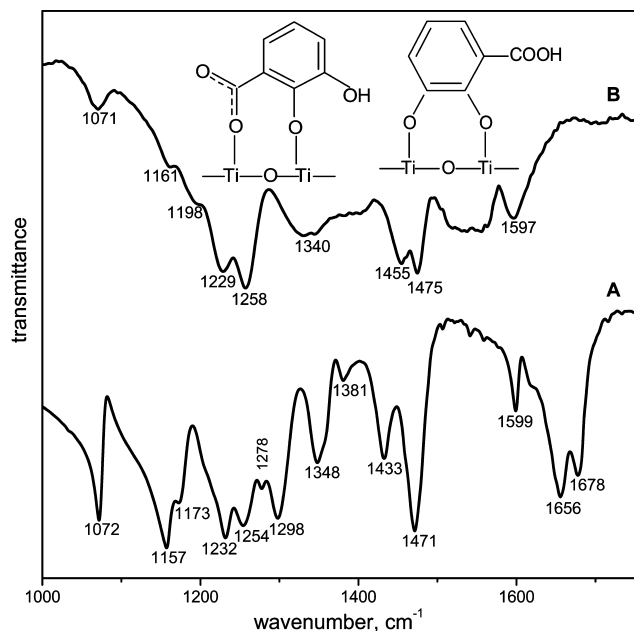


**Figure 8.** FTIR spectra of 2,3-DHBA: free (A) and adsorbed on TiO<sub>2</sub> nanoparticles (B) with proposed binding structure.

affects vibration bands in the region 1200–1300 cm<sup>-1</sup>, and only the pronounced band at 1278 cm<sup>-1</sup> is left. Since  $\nu(\text{C}=\text{O})$  at 1666 cm<sup>-1</sup> band still exists in ATR-FTIR spectrum of the complex, one may conclude that carboxylic group is still protonated not participating in the formation of the complex. The strong band at 1278 cm<sup>-1</sup> is very probably stretching or bending vibration of CO in COOH. The formation of the charge transfer complex also affects the ring frequencies, that is,  $\nu(\text{C}-\text{C})/\nu(\text{C}=\text{C})$  bands in the region 1400–1600 cm<sup>-1</sup> are shifted. All this indicates the presence of catechol type of binding with two oxygens of the phenolic groups coordinated to Ti surface atoms, the result quite expected having in mind the molecular structure of 3,4-DHBA. Although bidentate mononuclear chelate<sup>49,54</sup> is proposed as the way of binding, according to the Job's curve (not presented in Figure 3 for 3,4-DHBA) molar ratio between Ti<sub>surf</sub> atoms and 3,4-DHBA in the complex was found to be 2:1, and we find bidentate binuclear (bridging) complex more probable.

The ATR-FTIR spectra of 2,3-dihydroxybenzoic (3-hydroxy-salicylic) acid, free and adsorbed on TiO<sub>2</sub> nanoparticles, were presented in Figure 8. The main bands and their assignments<sup>49,55</sup> in free (protonated) acid (curve A) are as follows: stretching vibrations of the aromatic ring  $\nu(\text{C}-\text{C})/\nu(\text{C}=\text{C})$  at 1599, 1471, and 1433 cm<sup>-1</sup>, stretching vibrations of the phenolic group  $\nu(\text{C}-\text{OH})$  at 1278 and 1254 cm<sup>-1</sup>, bending vibrations of the phenolic group  $\delta(\text{C}-\text{OH})$  at 1381, 1348, and 1298 cm<sup>-1</sup>, bending  $\delta(\text{C}-\text{H})$  at 1173, 1157, and 1072 cm<sup>-1</sup>, stretching and bending vibrations of CO in COOH at 1232 cm<sup>-1</sup>, and the doublet at 1656/1678 cm<sup>-1</sup> assigned to stretching vibration of the carbonyl group  $\nu(\text{C}=\text{O})$ . The adsorption of 2,3-dihydroxybenzoic acid onto TiO<sub>2</sub> nanoparticles (curve B) leads to complete disappearance of the bands at 1381 and 1298 cm<sup>-1</sup> assigned to  $\delta(\text{C}-\text{OH})$  in the phenolic group, as well as the doublet at 1656/1678 cm<sup>-1</sup> assigned to  $\nu(\text{C}=\text{O})$  of the carboxylate group. The change in the intensity of the band assigned to vibrations of CO in COOH at 1232 cm<sup>-1</sup> is also observed. Ring frequencies are affected by the new environment, that is,  $\nu(\text{C}-\text{C})/\nu(\text{C}=\text{C})$  bands are shifted, indicating that the formation of a new ring makes different electronic distribution propagating to the whole aromatic ring. The results obtained prove both phenolic and

carboxylic group take part in chelation of titanium atoms. Since 2,3-dihydroxybenzoic acid contains three adjacent potential binding sites, surface complexation with metal atoms can be achieved through two adjacent OH groups (catecholate type) or and OH group in ortho position to the COOH group (salicylate type). The preferential type of binding is of course governed by formation of the energetically more favorable structure or steric hindrances.

#### 4. Conclusions

All investigated ligands (2-hydroxybenzoic acid, 2,3-dihydroxybenzoic acid, 2,5-dihydroxybenzoic acid, 3,4-dihydroxybenzoic acid, and catechol) form inner-sphere charge-transfer complexes with TiO<sub>2</sub> nanoparticles ( $d = 45 \text{ \AA}$ ). Binding of the modifier molecules to undercoordinated surface Ti atoms (defect sites) results in a significant change in the onset of absorption and the effective band gap. From the Benesi–Hildebrand plot, the stability constants at pH 2 of the order  $10^3 \text{ M}^{-1}$  have been determined. For chosen endiol modifiers, binding was found to be through bidentate binuclear (bridging) complexes leading to restoration of six-coordinated octahedral geometry of surface Ti atoms. Salicylate type (OH, COOH) of binding is characteristic for 2-HBA and 2,5-DHBA; catecholate type (OH, OH) is obvious in CAT and 3,4-DHBA, while both salicylate and catecholate type may participate in the binding of 2,3-DHBA. It is obvious that choosing the proper ligand can result in fine-tuning of the electronic properties of TiO<sub>2</sub>. Stabilized charge separation, being important feature of these systems opens-up possibility for using modifier molecules as conductive leads that allow electronic linking of the nanoparticle into molecular circuits providing further extension of photoinduced electron transfer.

**Acknowledgment.** Financial support for this study was granted by the Ministry of Science and Technological Development of the Republic of Serbia (Project 142066).

#### References and Notes

- Hagfeldt, A.; Grätzel, M. *Chem. Rev.* **1995**, *95*, 49.
- Grätzel, M. *Nature* **2001**, *414*, 338.
- O'Regan, B.; Grätzel, M. *Nature (London)* **1991**, *353*, 737.
- Nozik, A. J. *Annu. Rev. Phys. Chem.* **1978**, *29*, 189.
- Šaponjić, Z. V.; Dimitrijević, N. M.; Tiede, D. M.; Goshe, J. A.; Zuo, X.; Chen, L. X.; Barnard, A. S.; Zapol, P.; Curtiss, L.; Rajh, T. *Adv. Mater.* **2005**, *17*, 965.
- Rajh, T.; Chen, L. X.; Lukas, K.; Liu, T.; Thurnauer, M. C.; Tiede, D. M. *J. Phys. Chem. B* **2002**, *106*, 10543.
- Chen, L. X.; Rajh, T.; Jäger, W.; Nedeljkovic, J.; Thurnauer, M. C. *J. Synchrotron Rad.* **1999**, *6*, 445.
- Farges, F.; Brown, G. E., Jr.; Rehr, J. J. *Geochim. Cosmochim. Acta* **1996**, *60*, 3023.
- Dimitrijević, N. M.; Šaponjić, Z. V.; Bartels, D. M.; Thurnauer, M. C.; Tiede, D. M.; Rajh, T. *J. Phys. Chem. B* **2003**, *107*, 7368.
- Rajh, T.; Nedeljković, J. M.; Chen, L. X.; Poluektov, O.; Thurnauer, M. C. *J. Phys. Chem. B* **1999**, *103*, 3515.
- Moser, J.; Punchihewa, S.; Infelta, P. P.; Grätzel, M. *Langmuir* **1991**, *7*, 3012.
- Rajh, T.; Tiede, D. M.; Thurnauer, M. C. *J. Non-Cryst. Solids* **1996**, *205–207*, 815.
- Persson, P.; Bergström, R.; Lunell, S. *J. Phys. Chem. B* **2000**, *104*, 10348.
- Rajh, T.; Šaponjić, Z.; Liu, J.; Dimitrijević, N. M.; Scherer, N. F.; Vega-Arroyo, M.; Zapol, P.; Curtiss, L. A.; Thurnauer, M. C. *Nano Lett.* **2004**, *4*, 1017.
- Dimitrijević, N. M.; Šaponjić, Z. V.; Rabatić, B. M.; Rajh, T. *J. Am. Chem. Soc.* **2005**, *127*, 1344.
- Tunesi, S.; Anderson, M. *J. Phys. Chem.* **1991**, *95*, 3399.
- Martin, S. T.; Kesselman, J. M.; Park, D. S.; Lewis, N. S.; Hoffman, M. R. *Environ. Sci. Technol.* **1996**, *30*, 2535.
- Rodriguez, P.; Blesa, M. A.; Regazzoni, A. E. *J. Colloid Interface Sci.* **1996**, *177*, 122.



- (19) Regazzoni, A. E.; Mandelbaum, P.; Matsuyoshi, M.; Schiller, S.; Bilmes, S. A.; Blesa, M. A. *Langmuir* **1998**, *14*, 868.
- (20) Liu, Y.; Dadap, J. I.; Zimdars, D.; Eiseenthal, K. B. *J. Phys. Chem. B* **1999**, *103*, 2480.
- (21) Robert, D.; Parra, S.; Pulgarin, C.; Krzton, A.; Weber, J. V. *Appl. Surf. Sci.* **2000**, *167*, 51.
- (22) Roddick-Lanzilotta, A. D.; McQuillan, A. J. *J. Colloid Interface Sci.* **2000**, *227*, 48.
- (23) Weisz, A. D.; Regazzoni, A. E.; Blesa, M. A. *Solid State Ionics* **2001**, *143*, 125.
- (24) Weisz, A. D.; Garcia Rodenas, L.; Morando, P. J.; Regazzoni, A. E.; Blesa, M. A. *Catal. Today* **2002**, *76*, 103.
- (25) Heyd, D. V.; Au, B. *J. Photochem. Photobiol. A: Chem.* **2005**, *174*, 62.
- (26) Araujo, P. Z.; Mendive, C. B.; Garcia Rodenas, L. A.; Morando, P. J.; Regazzoni, A. E.; Blesa, M. A.; Bahnemann, D. *Coll. Surf. A* **2005**, *265*, 73.
- (27) Araujo, P. Z.; Morando, P. J.; Blesa, M. A. *Langmuir* **2005**, *21*, 3470.
- (28) Johnson, A. M.; Trakhtenberg, S.; Cannon, A. S.; Warner, J. C. *J. Phys. Chem. A* **2007**, *111*, 8139.
- (29) Tunesi, S.; Anderson, M. A. *Langmuir* **1992**, *8*, 487.
- (30) Dobson, K. D.; McQuillan, A. J. *Spectrochim. Acta A* **2000**, *56*, 557.
- (31) Connor, P. A.; Dobson, K. D.; McQuillan, A. J. *Langmuir* **1995**, *11*, 4193.
- (32) Dimitrijević, N. M.; Poluektov, O. G.; Šaponjić, Z. V.; Rajh, T. *J. Phys. Chem. B* **2006**, *110*, 25392.
- (33) Rajh, T.; Ostafin, A. E.; Micic, O. I.; Tiede, D. M.; Thurnauer, M. C. *J. Phys. Chem.* **1996**, *100*, 4538.
- (34) Eisenberg, G. M. *Ind. Eng. Chem. Anal.* **1943**, *15*, 327.
- (35) Chen, L. X.; Rajh, T.; Wang, Z.; Thurnauer, M. C. *J. Phys. Chem. B* **1997**, *101*, 10688.
- (36) Vosburgh, W. C.; Copper, G. R. *J. Am. Chem. Soc.* **1941**, *63*, 437.
- (37) Borgias, B. A.; Cooper, S. R.; Koh, Y. B.; Raymond, K. N. *Inorg. Chem.* **1984**, *23*, 1009.
- (38) Hultquist, A. E. *Anal. Chem.* **1964**, *36*, 149.
- (39) Hines, E. D.; Boltz, F. *Anal. Chem.* **1952**, *24*, 947.
- (40) Serpone, N.; Pelizzetti, E. *Photocatalysis. Fundamentals and Application*; Wiley Interscience: New York, 1989.
- (41) Tae, E. L.; Lee, S. H.; Lee, J. K.; Yoo, S. S.; Kang, E. J.; Yoon, K. B. *J. Phys. Chem. B* **2005**, *109*, 22513.
- (42) Günes, S.; Marjanović, N.; Nedeljković, J. M.; Sariciftci, N. S. *Nanotechnology* **2008**, *19*, 424009.
- (43) Benesi, H. A.; Hildebrand, J. H. *J. Am. Chem. Soc.* **1949**, *71*, 2703.
- (44) Person, W. B. *J. Am. Chem. Soc.* **1965**, *87*, 167.
- (45) Yost, E. C.; Tejedor-Tejedor, M. I.; Anderson, M. A. *Environ. Sci. Technol.* **1990**, *24*, 822.
- (46) Jiang, L.; Gao, L.; Liu, Y. *Colloids Surf., A* **2002**, *211*, 165.
- (47) Guan, X.; Chen, G.; Shang, C. *J. Environ. Sci.* **2007**, *19*, 438.
- (48) Biber, M. V.; Stumm, W. *Environ. Sci. Technol.* **1994**, *28*, 763.
- (49) Guan, X.; Shang, C.; Chen, G. *Chemosphere* **2006**, *65*, 2074.
- (50) Jadrijević-Mladar Takač, M.; Vikić Topić, D. *Acta Pharm.* **2004**, *4*, 177.
- (51) Vega-Arroyo, M.; LeBreton, P. R.; Rajh, T.; Zapol, P.; Curtiss, L. A. *Chem. Phys. Lett.* **2005**, *406*, 306.
- (52) Redfern, P. C.; Zapol, P.; Curtiss, L. A.; Rajh, T.; Thurnauer, M. C. *J. Phys. Chem. B* **2003**, *107*, 11419.
- (53) Ayinde, B. A.; Onwukaeme, D. N.; Omogbai, E. K. *Acta Pol. Pharm., Drug Res.* **2007**, *64*, 183.
- (54) Karaliota, A.; Kamariotaki, M.; Hadjipanagioti, D.; Aletras, V. *J. Inorg. Biochem.* **1998**, *69*, 79.
- (55) Aletras, V.; Karaliota, A.; Kamariotaki, M.; Hatzipanayioti, D.; Hadjiliadis, N. *Inorg. Chim. Acta* **2001**, *312*, 151.

JP9013338